JOURNAL OF MATERIALS SCIENCE 32 (1997) 1599–1602

$Li_3B_5O_8(OH)_2$: crystal growth and ionic conductivity studies

K. BYRAPPA, V. P. JAYANTHARAJA, K. V. K. SHEKAR, V. RAJEEV*, V. J. HANUMESH*, A. R. KULKARNI††, A. B. KULKARNI*
*Department of Geology, University of Mysore, Manasagangotri, Mysore 570 006, India and *Department of Applied Electronics, Gulbarga University, Gulbarga 585 106, Karnataka, India and ††Department of Metallurgical Engineering and Materials Science, Indian Institute of Technology, Powai, Bombay-400 076, India.*

$Li_3B_5O_8(OH)_2$ crystals were grown using hydrothermal techniques applied to the system $Li_2O–B_2O_3–H_2O$. Detailed ionic conductivity measurements have been performed.

1. Introduction

Alkali borates constitute an important group of technologically interesting materials that display a wide range of physical and chemical properties. These physico-chemical properties are essentially due to the atomic arrangement which consists of $[BO_3]$ triangles and $[BO_4]$ tetrahedra [1]. Initial investigations of the $Li_2O–B_2O_3$ system began in the middle of this century [2] and the recent growth in interest in these materials is due to the use of hydrothermal conditions to obtain high quality samples. The present authors have investigated the $Li_2O–B_2O_3–H_2O$ system in detail using the hydrothermal technique and obtained many new alkali borate compounds. The phase diagram for the system, $Li_2O–B_2O_3–H_2O$ shows that the following phases can be synthesized using the hydrothermal conditions of a pressure of 1×10^7 Pa at a temperature of 250 °C: $Li_2B_4O_7$, $Li_3B_5O_8(OH)_2$, $Li_4B_7O_{12}Cl$, Li_2HBO_3 and $LiH_2B_5O_9$ [3].

In this paper, the growth of crystals of $Li_3B_5O_8(OH)_2$ is investigated and measurements on the ionic conductivity of this material are also reported.

2. Experimental procedure

2.1. Crystal growth

The growth of alkali borates can be achieved using one of several methods such as the flux, melt, sol–gel and hydrothermal techniques. The flux method is one of the earliest and most extensively used methods for the growth of not only alkali borates but also several other mixed borates. Similarly the melt technique is a popular technique for the growth of alkali borates, particularly lithium tetraborate and lithium triborate. Crystals of $Li_3B_5O_8(OH)_2$ have to date only been grown by the hydrothermal technique. It is only during the last decade that we have gained detailed insights into the behaviour of boron in hydrothermal solutions and its interaction with various metal cations.

The growth experiments were carried out using a Morey type of autoclave (15–20 cm in length and 6 cm in diameter, fabricated at the Department of Geology, Mysore University) provided with Teflon liners. The crystallization was carried out through spontaneous nucleation. The type and rate of nucleation are functions of (i) the composition and concentration of the solution, (ii) temperature, (iii) pressure (% filling), (iv) hydrodynamic conditions, and (v) surface contact of the solid and liquid phases. In the system $Li_2O–B_2O_3–H_2O$, the title compound crystallizes within a narrow region. Any slight change in the growth parameters can change the resultant products as can be observed from Fig. 1. The formation of $Li_3B_5O_8(OH)_2$ takes place via the following reactions:

$$LiOH + H_3BO_3 \rightarrow LiBO_2 + 2H_2O \quad (1)$$

$$3LiBO_2 + 2H_3BO_3 \rightarrow Li_3B_5O_8(OH)_2 + 2H_2O \quad (2)$$

In Fig. 2 we show a representative photograph of a $Li_3B_5O_8(OH)_2$ crystal grown in this work. The size of crystals obtained using the hydrothermal technique varies from 1–14 mm. Usually the crystals were well developed with a good morphology and in addition twinning was uncommon. On the whole, $Li_3B_5O_8(OH)_2$ crystals display some very unusual growth features (Fig. 3) that are absent in other alkali borates [4].

2.2. Ionic conductivity

The $Li_3B_5O_8(OH)_2$ crystals were characterized using a number of techniques such as X-ray diffraction, chemical analysis, and Differential thermal analysis. In addition the morphology of the crystals was studied and also preliminary ionic conductivity studies were performed. The results of these characterization studies have been published elsewhere [4–6]. The structure of the $Li_3B_5O_8(OH)_2$ crystals [7] and preliminary ionic conductivity measurements [5] show that these crystals exhibit poor ionic conductivity with the

0022–2461

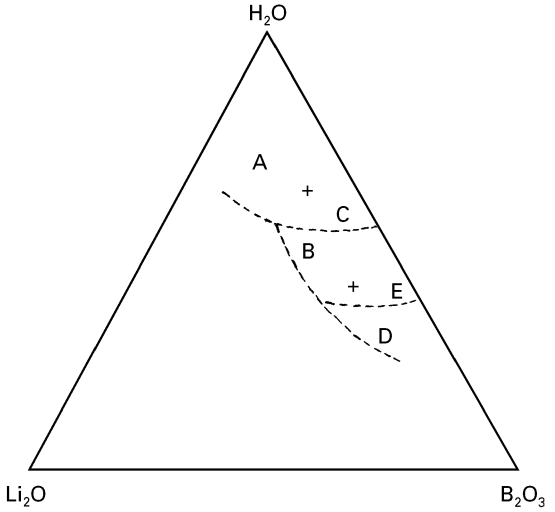

Figure 1 Phase diagram for the system Li_2O–B_2O_3–H_2O. Compounds: this system are (A) $Li_4B_7O_{12}Cl$, (B) $Li_2B_4O_7$, (C) $Li_3B_5O_8(OH)_2$ (D) $Li_2H_2B_5O_9$ and (E) Li_2HBO_3.

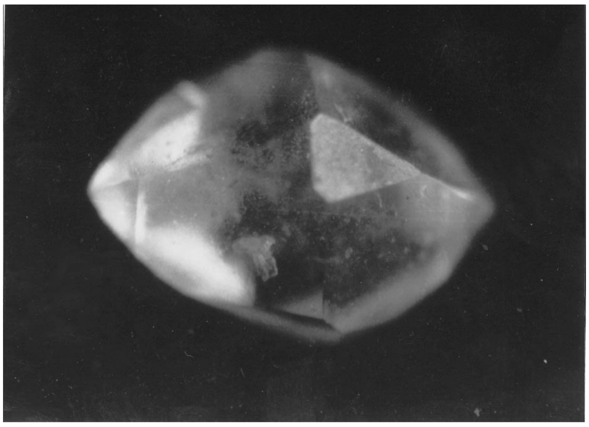

Figure 2 Representative photograph of a $Li_3B_5O_8(OH)_2$ crystal obtained by the hydrothermal method. Magnification (× 7.2).

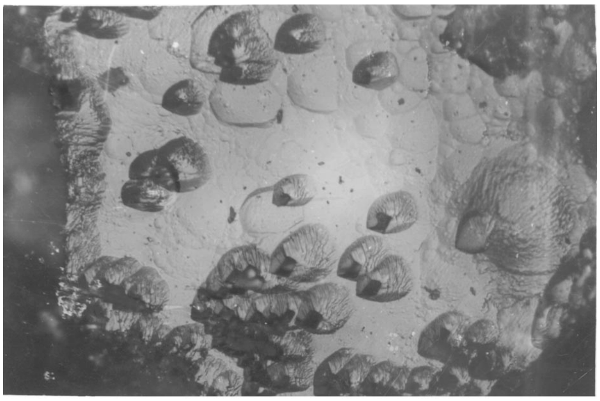

Figure 3 Characteristic surface morphology of $Li_3B_5O_8(OH)_2$ crystals. Magnification (× 72).

material behaving as a dielectric below 498 K. The complex impedance spectroscopic (CIS) plots show scattered data points over a wide frequency range. When data is obtained near the origin, one obtains a vertical spike parallel to the imaginary axis. This represents a pure capacitor as modeled by an electronic equivalent circuit. Since this material shows both a dielectric and superionic nature, we have carried out detailed CIS studies on the $Li_3B_5O_8(OH)_2$ crystals.

The detailed CIS measurements for $Li_3B_5O_8(OH)_2$ have not been previously reported in the literature. Systematic CIS measurements have been carried out using a Solartron Impedance/Gain Phase analyser system (Model 1260, Germany) in the frequency range 1 Hz to 32 MHz. The temperature was varied from 299–573 K. The impedance analyser system was interfaced to PC/AT-486 through a general purpose interface bus for automated data acquisition. The CIS data was measured at 150 software selected points in the said frequency range.

The polycrystalline material was powdered and pressed into pellets at a pressure of 5 ton cm^{-2}. The pellet had a diameter of 10 mm and a thickness of 2 mm. Screw loaded silver metallic electrodes were positioned on both sides of the pellet. The density of the pellet was 85% of theoretical density. The pellets were prepared 60 days after the synthesis and the CIS measurements were carried out a further 20 days after the pelletization. The data was analysed using the Equivalent Circuits Program [8]. The measured CIS data is displayed in Fig. 4(a–l). At 299 K, the expanded data near the origin of the complex impedance plot, shows a vertical line parallel to the imaginary axis (inset of Fig. 4a). This indicates a pure capacitor in the electronic equivalent circuit representation. This behaviour continues between 299–398 K. At 423 K, the CIS data is an approximate semi-circle and a spike in the complex impedance plane (Fig. 4f). Obviously there is a considerable amount of noise in the lower frequency region. A systematic study of the source of this noise and its statistical analysis is currently in progress and will be published at a later date. From 448–498 K, a capacitor type of behaviour is repeated. From 523–573 K, the CIS data shows a depressed semi-circle with a spike. There is an appreciable amount of noise in the data taken at 523 K in the lower frequency region, particularly in the spike region. This noise decreases as the frequency (f) increases, hence it may be a quantum noise or $1/f$ noise. This noise is generally observed in the spike region which represents an electrode phenomenon. This depressed semi-circle has a diameter below the real axis which implies a distribution of the relaxation time. The bulk resistance (R_b) has been determined from the impedance plot and from these B_b values, the bulk conductivities (σ_b) have been calculated. From 299–523 K, the material exhibits piezoelectric behaviour and at about 523 K it shows a superionic nature. The complex impedance is represented by $Z^* = Z' - jZ''$. In Fig. 5(a–d) the Bode plots ($\ln Z'$ versus $\log f$ and $\ln Z''$ versus $\log f$) at 299 K for the entire frequency range are plotted Z'' is found to decrease linearly with frequency and there is a sharp dip at 10 MHz. Z' decreases continuously and finally at 10 MHz, there is a sharp dip. This reveals that the complex impedance becomes almost zero at 10 MHz. Therefore, a device with this material will resonate at 10 MHz and the resonance is quite sharp.

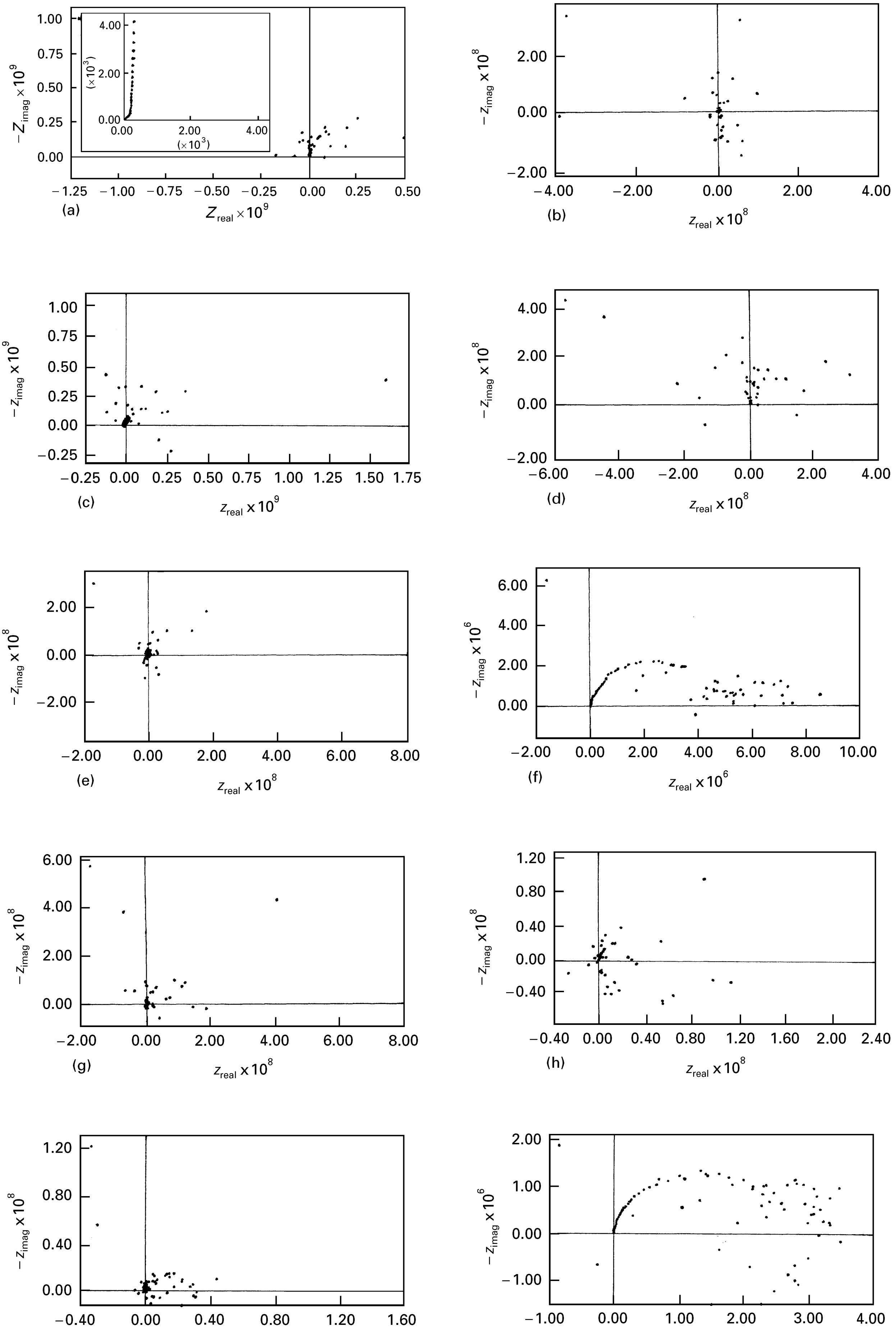

Figure 4 (a–l) Complex impedance plots of $Li_3B_5O_8(OH)_2$ crystals at the temperatures: (a) 299 K, (b) 323 K, (c) 348 K, (d) 373 K, (e) 398 K, (f) 423 K, (g) 448 K, (h) 473 K, (i) 498 K, (j) 523 K, (k) 548 K and (l) 573 K respectively. Here Z' and Z'' denote Z_{real} and Z_{imag} respectively of the text.

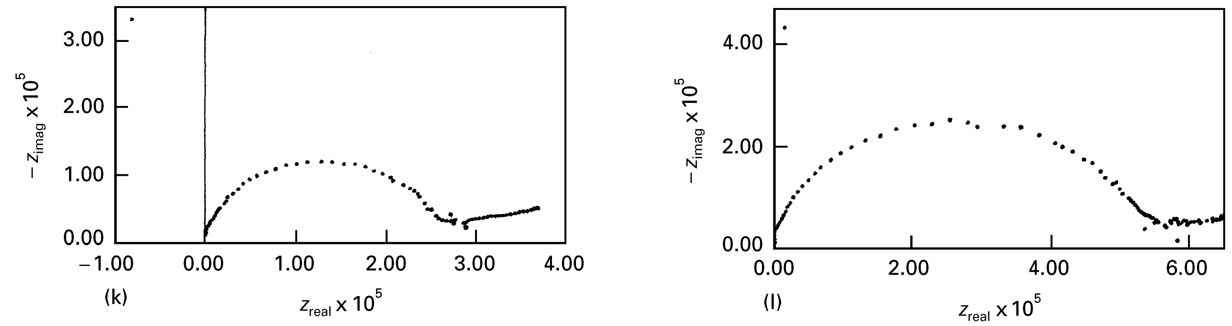

Figure 4 Continued.

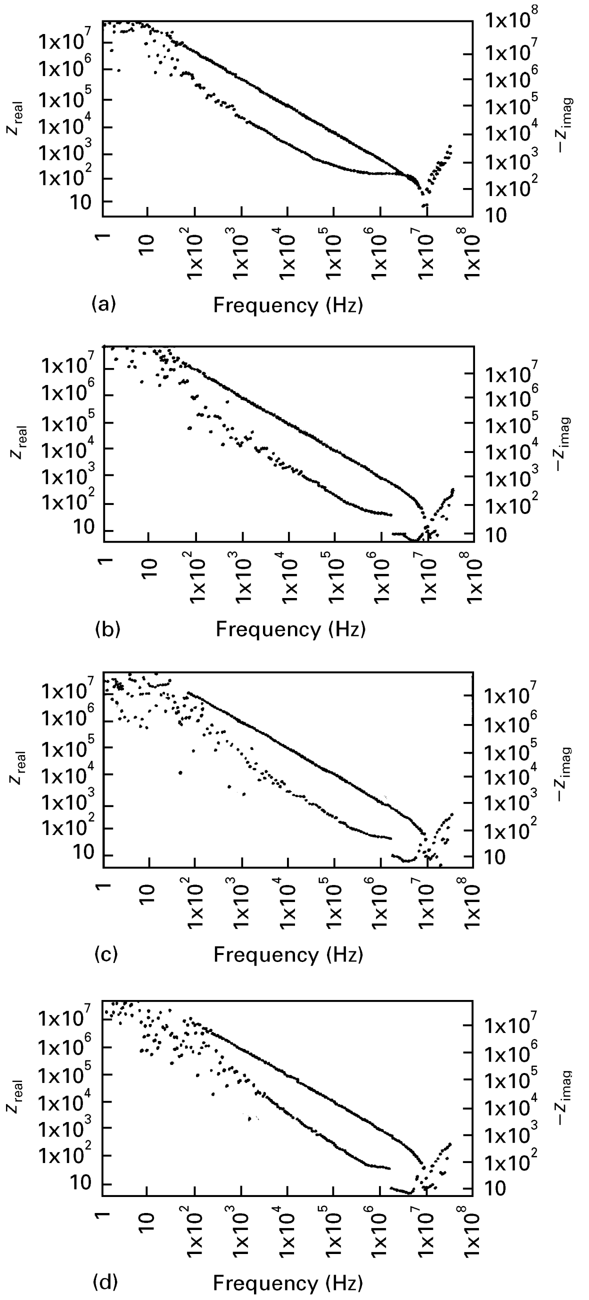

Figure 5 (a–d) Representative Bode plots of $Li_3B_5O_8(OH)_2$ crystals showing variation of Z' and Z'' as function of frequency (a) at 299 K, (b) at 323 K, (c) at 348 K and (d) at 373 K.

There is an appreciable amount of noise up to 1 KHz in case of Z'. This noise decreases as the frequency increases. The noise also decreases as the temperature increases in the range 299–398 K and ceases when the temperature is raised further. Therefore, the noise is not purely due to thermal effects, it is in fact a quantum noise or $1/f$ noise. To sum up; $Li_2B_5O_8(OH)_2$ behaves as a piezoelectric material which resonates at 10 MHz and between 523–573 K it displays a superionic nature.

3. Conclusions

(1) $Li_3B_5O_8(OH)_2$ crystals were obtained using a hydrothermal technique.

(2) The composition and concentration of the solution, temperature, pressure (% filling), hydrodynamic conditions and surface contact of the solid and liquid phases helped to determine the type and rate of the nucleation.

(3) $Li_3B_5O_8(OH)_2$ crystals display some very unusual growth features that are absent in many other alkali borates.

(4) $Li_3B_5O_8(OH)_2$ shows poor ionic conductivity and behaves as a dielectric material below 498 K, with the electronic equivalent circuit representation indicating a pure capacitor type behaviour.

(5) Between 299–523 K, the material exhibits piezoelectric behaviour and at about 523 K it shows superionic conducting behaviour.

(6) The complex impedance becomes almost zero at 10 MHz.

Acknowledgements

This work was financed by BRNS, Department of Atomic Energy, Government of India.

References

1. A. S. POVERENNYKH, "Crystal Chemical Classification of Minerals," Vol. 1 (1972) p 156.
2. B. S. R. SASTRY and F. A. HUMMEL, *J. Amer. Ceram. Soc.* **41** (1958) 7.
3. K. BYRAPPA and K. V. K. SHEKAR, *J. Mater. Res.* **8** (1993) 864.
4. K. BYRAPPA, K. V. K. SHEKAR and R. RODRIGUEZ CLEMENTE, *ibid.* **8** (1993) 2319.
5. K. BYRAPPA, K. V. K. SHEKAR and S. GALI, *Cryst. Res. Tech.* **27** (1992) 767.
6. K. V. K. SHEKAR, Ph.D. thesis, Mysore University, Mysore (1993).
7. O. S. BONDARAVA, Y. K. EGOROV-TISMENKO and N. V. SIMONOV, *Sov. Phys. Dokl.* **23** (1978) 806.
8. B. A. BOUKAMP, Equivalent Circuit Users Manual, University of Twente. The Netherlands, May 1989.

Received 21 August 1995
and accepted 13 June 1996